Materials Characterization 141 (2018) 163–168

Contents lists available at ScienceDirect

Materials Characterization

journal homepage: www.elsevier.com/locate/matchar

Effect of aging treatment on microstructures, tensile properties and intergranular corrosion behavior of Al–Cu–Li alloy

Yi Lin[a,b,*], Change Lu[c], Chengyang Wei[d], Ziqiao Zheng[e]

[a] Analytical and Testing Center, Sichuan University of Science & Engineering, Zigong 643000, PR China
[b] School of Materials Science and Engineering, Sichuan University of Science & Engineering, Zigong 643000, PR China
[c] College of Chemistry and Environmental Engineering, Sichuan University of Science & Engineering, Zigong 643000, PR China
[d] Advanced Metal Materials Research Laboratory, Guangdong Zhaoqing Institute of Quality Inspection & Metrology, Zhaoqing 526000, PR China
[e] School of Materials Science and Engineering, Central South University, Changsha 410083, PR China

ARTICLE INFO

Keywords:
Al–Cu–Li alloy
Aging treatment
Microstructures
Tensile properties
Intergranular corrosion

ABSTRACT

The influence of aging treatment on microstructures, tensile properties and corrosion properties of Al–Cu–Li alloy was investigated. The results show that the T8 duplex aging treatment was more effective than T6 and T8 single aging treatment in enhancing the tensile properties and improving the intergranular corrosion (IGC) resistance. Based on the microstructure observation, tensile test, electrochemical experiment and IGC measurement, the factors which affect the microstructures, tensile properties and IGC behavior changing of Al–Cu–Li alloy during aging treatments were discussed in detail.

1. Introduction

Weight reduction, lifetime prolongation, customer satisfaction and environmental friendliness are mainly technology driving force of aircraft industry. Due to the great effort of aircraft and aluminum industries, Al–Cu–Li alloy has been developed as an alternative solution for the design and fabrication of new generation aircraft. The attractive properties of this series Al alloy associate with the addition of Li, which not only bring about significant weight reduction but also enable the alloy to attain higher elastic modulus, lower density, higher specific strength and more favorable damage tolerance properties compared with those of traditional 2xxx and 7xxx series Al alloy [1–3].

The Al–Cu–Li alloy is one of age–hardenable alloys. Depending on the chemical composition, the main strengthening phases of the alloy can be T_1 (Al_2CuLi), θ' (Al_2Cu), S' (Al_2CuMg) and δ' (Al_3Li) [4,5]. Other minor elements, such as Ag, Sc, Zr and Zn, are usually added to the alloy to form dispersoid particles (e.g., Al_3Sc and Al_3Zr), which are able to accelerate the precipitation of strengthening phases, improve corrosion resistance and increase thermal stability of alloy [6,7].

The type and morphology of precipitates in the Al–Cu–Li alloy are also strongly affected by the thermo–mechanical processing. In recent years, many works have been carried out to study the influence of various processing methods on the microstructures and properties of Al–Cu–Li alloy. Zhang et al. pointed out that icosahedral quasicrystalline phase T_2 (Al_6CuLi_3) formed in the grain boundaries of laser–welded 2060 alloy with lower Li content as a result of segregation and replacement of Mg element [8]. Li et al. showed that aging–forming inhibited the precipitation of θ' phases, promoted precipitation of T_1 phases and reduced the dimension of T_1 phases, and this in turn enhanced the mechanical properties and improved the corrosion resistance of Al–Cu–Li alloy [9]. Jia et al. found that the coarse continuous AlCu phases precursor in the as–cast 1469 alloy dissolved and broken off during homogenization, and transformed into the W (AlCuSc) phases [10]. Benoit et al. observed that the precipitation kinetics of different phases in the welding zones of 2050 alloy joint was mainly controlled by the local dislocation density inherited from friction stir welding [11]. These pioneer works manifest that a great variety of precipitates in the Al–Cu–Li alloy is prone to induce the microstructural evolution behavior to be different during thermo–mechanical processing as slight modification of chemical composition, leading to significant variation in mechanical properties, corrosion resistance, thermal stability or welding performance. Meanwhile, the interaction of these phases would make the relationship between precipitate and material properties to be more complex in comparison with that of conventional Al alloy, which greatly increases the difficulty in controllable fabrication of microstructure and properties of Al–Cu–Li alloy. Therefore, investigation the influence of thermal–mechanical processing on the microstructure and properties of Al–Cu–Li alloy is still necessary, which is beneficial to ascertain the relation between microstructures and processing methods, develop new processing technique

* Corresponding author at: Analytical and Testing Center, Sichuan University of Science & Engineering, Zigong 643000, PR China.
E-mail address: llinyi@163.com (Y. Lin).

https://doi.org/10.1016/j.matchar.2018.04.043
Received 24 September 2017; Received in revised form 1 April 2018; Accepted 24 April 2018
Available online 25 April 2018
1044-5803/

and explore the application potentiality of alloy. The present work was undertaken to investigate the effect of aging treatment on microstructures, mechanical properties and IGC behavior of Al–Cu–Li alloy, and uncover the corresponding microstructures and properties evolution mechanisms. These results can give indispensable information for optimizing the properties and processing techniques of Al–Cu–Li alloy.

2. Experimental

The experimental material Al–2.58Cu–1.64Li–0.32 Mg–0.67Zn–0.35Mn (wt%) was prepared by liquid metallurgy route. The as–cast alloy was homogenized in a salt bath, and then extruded into a cylindrical rod of 18 mm diameter at 470 °C. After that, the extruded rod was machined into tensile samples with lengths of 100 mm. These samples were heat treated to obtain T6 and T8 temper, respectively. The T6 temper was developed by solutionizing at 540 °C for 1 h, quenching in water and aging at 175 °C. The T8 temper was achieved by solution heat treatment at 540 °C for 1 h followed by water quenching, 2.5% pre–deformation, and single aging at 150 °C or duplex aging at 120 °C for 12 h and then at 150 °C for a certain time.

The hardness was tested by a hardness tester (VMH–002UD), and three samples of each group were measure. The tensile test was performed on MTS 858 testing machine in a displacement–controlled mode at a displacement rate of 2 mm/min. An extensometer attached to the sample gauge was used to determine strain and total elongation. After tensile test, the fracture surface of specimen was observed by scanning electron microscope (SEM, Quanta 200).

IGC test was performed in a solution of 0.97 mol/L NaCl + 10 mL H_2O_2 at about 25 °C for 24 h, and five samples of each condition were tested. The corrosion behavior of the samples was studied using conventional immersion test and stationary electrochemical technique. For immersion test, only one surface of the sample with dimension of 10 mm × 10 mm was exposed to the solution, while the other planes were encapsulated by epoxy. After immersion, the sample was cleaned with deionized water and dried. The areas of corrosion attack in the exposed surface were located at a magnification of 10 times. Afterward, the cross section of sample was grind by abrasive paper and polished by diamond paste, subsequently the extent of IGC was characterized by SEM.

Electrochemical test was carried out using a three–electrode electrochemical system, including a platinum grid with a large surface area as the auxiliary electrode, a saturated calomel electrode (SCE) as the reference electrode and the sample with a square surface of 10 mm^2 as the working electrode. Potentiodynamic polarization test was conducted at 0.2 mV/s ranging from −1 V_{SCE} to 1 V_{SCE}. And all the measurements were performed in 3.5 wt% NaCl solution at room temperature.

The precipitates and morphology of grain boundary were characterized by transmission electron microscope (TEM, Tecnai G2 200). The foils for TEM observation were firstly taken from tensile samples and subsequently electro–thinned in a mixture of methanol and nitric acid at −25 °C. Statistical analysis of the TEM images was performed by ImageJ software to calculate the size and number density of strengthening phases using the automated particle detection function of the software, and all these statistical parameters were counted from at least 500 individual (i.e., non–touching) precipitates to avoid any influence from overlapping particles to the statistical results. In the statistical analysis process, each δ' phase was assumed to be spherical, and each T_1 phase was identified to be rectangular.

3. Results

3.1. Microhardness and Tensile Properties

The hardness curves of the samples treated by different aging treatments are shown in Fig. 1a. In the T6 aging condition, the hardness rose to peak value of 151 HV after aging at 175 °C for 32 h, and with further prolonging the aging time, the hardness decreased obviously. The hardness of T8 single aged sample increased from 78 HV to 157 HV within 44 h at 150 °C, and the hardness showed little change with aging time up to 200 h. In the T8 duplex aging state, the hardness slowly rose to 85 HV during the first step aging (12 h at 120 °C), and the peak–aged hardness value of 168 HV was attained after secondary aging at 150 °C for 48 h.

Fig. 1b shows the tensile properties of peak–aged samples in different aging conditions. In the T6 state, the yield strength and elongation were 519 MPa and 5.7%, respectively. The yield strength and elongation of T8 single aged sample were increased by 19% and 14% as compared with those of T6 aged sample. When the sample was treated by T8 duplex aging, the tensile properties was further improved, and the yield strength and elongation were 610 MPa and 7.8%, respectively. These results manifest that T8 aging was more effective in enhancing the strength of sample than T6 aging did, and the duplex aging was more suitable for improving the ductility.

The corresponding fracture surface SEM images of tensile samples are shown in Fig. 2. The T6 aged specimen exhibited brittle quasi–-cleavage fracture behavior predominated by large cleavage facets, meanwhile few of small dimples were kept at the fractured location (Fig. 2a). The fracture surface of T8 single aged sample exhibited smaller cleavage facets and more dimples in comparison with those of sample treated by T6 aging, representing that the specimen failed in dimples and quasi–cleavage mode (Fig. 2b). The sample undertaken T8 duplex aging also failed in the ductile–brittle mixed mode, but many deep and large dimples were observed in the fracture surface (Fig. 2c).

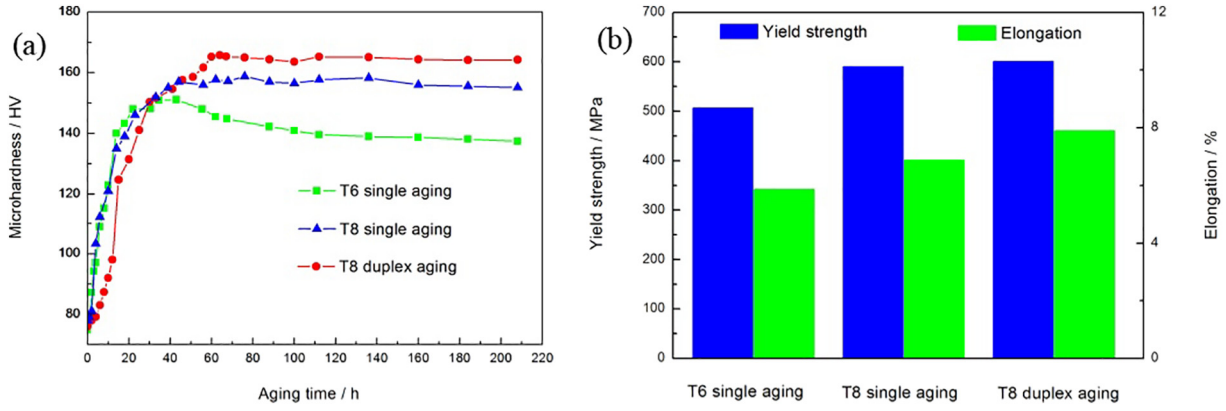

Fig. 1. Hardness curves (a), and tensile properties (b) of samples treated by different aging treatments.